Structural analogues of existing anti-viral drugs inhibit SARS-CoV-2 RNA dependent RNA polymerase: A computational hierarchical investigation

Md. Kamrul Hasan (kamrulhasanhridoy205@gmail.com)
Tejgaon College, National University of Bangladesh, Gazipur, Bangladesh https://orcid.org/0000-0002-3032-7640
Mohammad Kamruzzaman
University of Dhaka https://orcid.org/0000-0002-7954-673X
Omar Hamza Bin Manjur
University of Dhaka
Araf Mahmud
Shahjalal University of Science & Technology
Nazmul Hussain
Tejgaon College, National University of Bangladesh, Gazipur, Bangladesh
Muhammad Shafiul Alam Mondal
University of Dhaka
Md. Ismail Hosen
University of Dhaka https://orcid.org/0000-0003-0862-7206
Martiniano Bello
instituto politécnico nacional https://orcid.org/0000-0002-9686-0755
Atiqur Rahman
University of Dhaka https://orcid.org/0000-0003-0086-2586

Research Article

Keywords: COVID-19, RNA dependent RNA polymerase, binding free energy, Molecular docking, virtual screening, Molecular dynamics simulation

Posted Date: November 6th, 2020

DOI: https://doi.org/10.21203/rs.3.rs-103595/v1

Version of Record: A version of this preprint was published at Heliyon on March 1st, 2021. See the published version at https://doi.org/10.1016/j.heliyon.2021.e06435.

Abstract

It's been more than 8 months since COVID-19 became a pandemic and scientists all over the world are struggling to find suitable solutions to combat it. Multiple repurposed drugs have already been in several trials or recently completed. However, none of them shows any promising effect in combating COVID-19. Therefore, developing an effective drug is an unmet global need. RdRP (RNA dependent RNA polymerase) plays a pivotal role in viral replication therefore, it is considered as a prime target of drugs that may treat COVID-19. In this study, we have screened a library of compounds, containing approved RdRP inhibitor drugs in use to treat other viruses (Favipiravir, Sofosbuvir, Ribavirin, Lopinavir, Tenofovir, Ritonavir, Galidesivir and Remdesivir) and their structural homologues, in order to identify potential inhibitors of SARS-Cov-2 RdRP. Extensive screening, molecular docking and molecular dynamics show that five structural analogues have notable inhibitory effects against RdRP of SARS-Cov-2. Importantly, comparative protein-antagonists interaction revealed that these compounds fit well in the pocket of RdRP. ADMET analysis of these compounds suggests their potency as drug candidates. Our identified compounds may serve as potential therapeutics for COVID-19.

Introduction

SARS (Severe Acute Respiratory Syndrome)-Cov-2 is a novel coronavirus that first emerged in late 2019 at Wuhan of China (Ludwig and Zarbock, 2020). This is the 7th coronavirus species discovered, belonging to the order Nidovirales of the Coronaviridae family. Since its emergence, till 1st November 2020, it has reportedly infected 46,210,349 people and caused 1,197,805 deaths in total (Coronavirus Update (Live): 46,210,349 Cases and 1,197,805 Deaths from COVID-19 Virus Pandemic - Worldometer). Ever since the disease broke out in China, the whole world started taking precautionary measures but failed to stop its rapid spread across the globe. Due to its extreme outbreak, the World Health Organization (WHO) declared a state of emergency and called on a global pandemic on March 11, 2020 (Brinks and Ibert, 2020). Initially, the disease was characterized by fever, coughing, sneezing, shortness of breath, or breathing difficulties (Huang et al., 2020) though in severe cases the disease can result in pneumonia, multiple organ failure leading to death. Recent cases complaining of a higher rate of renal impairment indicates its possible role in rendering Kidney dysfunction (Li et al., 2020). Similar to an influenza outbreak, COVID-19 causes myocardial injury that may be related to increased viscosity, heightened coagulation cascade, pro-inflammatory effects, or endothelial cell dysfunction caused by SARS-CoV-2 virus (JC et al., 2018; Nguyen et al., 2016). The virus attaches to its host cell mostly in the upper respiratory tract via an interaction taking place between the virus's spike glycoprotein and human's ACE-2 receptor (Tai et al., 2020).

The molecular biology of this novel coronavirus has already been vividly studied and several salient features of its genome organization have been elucidated in a number of works. This RNA genome consists of at least six open reading frames (Ahmed et al., 2020). One Open Reading Frame of special importance is the ORF 1a/b which constitutes two-thirds of the whole genome and synthesizes two very important polypeptides namely polypeptide 1a and polypeptide 1ab which eventually produce the 16 Nonspecific proteins (NSPs) of the virus. The other 5 ORFs constitute nearly one-third of the genome and produce the four structural proteins for the virus, Spike Glycoprotein (S), Envelope Glycoprotein (E), Membrane protein (M) and Nucleoprotein (N) respectively (Woo et al., 2010). Eleven cleavage sites have so far been discovered for NSP5 and it generates many important proteins, including RdRP. RdRP can be a major target for anti-viral drug treatment. It plays crucial role in the replication of RNA viruses that makes it an ideal drug target for anti-viral drug development against RNA viruses. For treating many RNA virus infections such as Hepatitis C, Zika and several coronaviruses, many anti-viral drugs have already been developed which target the viral RdRP enzyme (Elfiky, 2020). Some antiviral drugs like Remdesivir, Favipiravir have been briefly tested against SARS-CoV-2 RdRP, though partially successful further validation is required for the clinical approval to use those for treating SARS-CoV-2 infection (Harrison, 2020; Lung et al., 2020; Zhang1 and Zhou1, 2020).

Over the last ten months, scientists have come up with different ways to alleviate the severity of the disease and reduce its contagiousness (Van Kampen et al., 2020). However, much of the hope is vested alone on the vaccines which are currently on phase-3 clinical trials (Slaoui and Hepburn, 2020). Since the development of effective vaccines is still uncertain and vaccination program covering the whole world population is a time requiring process, effective antiviral drugs would be an effective solution to combat this life-threatening infection. Since new drugs require a long time to come into the market, repurposing existing drugs would be a suitable alternative for effectively tackling the infection. The enzyme, RdRP plays a pivotal role in viral replication, having no host homologues and, therefore, developing therapeutics that inhibit the enzyme would not only inhibit viral replication but also can minimize any potential risks in host cells. A number of FDA-approved RdRP inhibitor drugs, which include Remdesivir, Favipiravir, Sofosbuvir, Ribavirin, Lopinavir, Ritonavir, Tenofovir and Galidesivir, are effective against a broad range of RNA viruses, including past coronaviruses (Li and De Clercq, 2020; Mitjà and Clotet, 2020; Şimşek Yavuz and Ünal, 2020; Sinha and Balayla, 2020). Although remdesivir, an experimental Ebola virus drug, has been approved for emergency use only for hospitalized patients and recent clinical data suggest a moderate clinical improvement by reducing the recovery period (Beigel et al., 2020), however, no impact on mortality; therefore, the potentiality of the drug is not as promising as expected. Therefore, identifying novel therapeutics that have the potential to effectively combat the disease is an unmet need. To address this, we, herein, virtually screened FDA approved RdRP inhibitor drugs and their structural analogues (~2400 compounds) based on molecular docking analysis of these compounds in order to identify drug candidates that can potentially inhibit SARS-CoV-2 RdRP. Based on docking scores, protein-ligand interactions, molecular dynamic simulations and free energy calculation we predicted five RdRP inhibitor drug candidates that may have the potential to combat life-threatening SARS-CoV-2 infection, and therefore, may serve as a cure to treat the disease, addressing the current global need.

Method

2.1. Ligand selection and preparation:

An extensive literature assessment was performed to gather information on antiviral drugs that target and inhibit RdRP enzyme. RdRP blocking abilities with various extents of effect in other RNA viruses (H1N11 (Lin et al., 2015), HCV2 (Hofmann et al., 2008), HIV3 (Blair and Cox, 2016), SARS (Fani et al., 2020) and MERS (Fani et al., 2020) have been reported by eight antiviral compounds: Favipiravir (Allen et al., 2020), Sofosbuvir (Buonaguro and Buonaguro, 2020),

Lopinavir (Chakraborty and Das, 2020), Tenofovir (Allen et al., 2020), Ribavirin (Gish, 2006), Ritonavir (Chakraborty and Das, 2020), Galidesivir (Allen et al., 2020) and Remdesivir (Fani et al., 2020) have been primarily reported to have. To determine their potential in inhibiting SARS CoV-2 RdRP computationally, their SDF (Spatial Data *File)* files were downloaded from the PubChem database (https://pubchem.ncbi.nlm.nih.gov/). Moreover, structurally similar compounds of the inhibitor drugs were downloaded from Swiss similarity software (Zoete et al., 2016) (http://www.swisssimilarity.ch/) by activating zinc drug-like features. A library of ~2400 compounds has been prepared.

2.2. Macromolecule selection and preparation:

The crystal structure of RNA dependent RNA polymerase (RdRP) was collected from the RCSB Protein Data Bank (https://www.rcsb.org/search) (PDB ID: 6M71) (Gao et al.) followed by optimization and processing of the structure by Swiss-PDB viewer software packages (Guex and Peitsch, 1997) (https://spdbv.vital-it.ch/) (version 4.1.0) based on their least energy. Some significant factors, such as side-chain geometry, improper bond order, and missing hydrogen, were observed in the crystal structure of the RdRP protein. PyMol (version 1.1) software package (Adams et al., 2010) (https://pymol.org/2/) was used to remove all the water molecules, hetero atoms, and inhibitor existent in the Crystal structure.

2.3. Virtual screening and ligand preparation

As mentioned above the structural analogues of the inhibitor drugs were obtained from the ZINC database (Sterling and Irwin, 2015) for the best optimal hit against the mentioned target (**Figure 1**). PyRx (Dallakyan and Olson, 2015) from MGLTools (https://ccsb.scripps.edu/mgltools/) is used here. For Computational Drug Discovery, PyRx is used as a Virtual Screening software. It screens libraries of compounds against potential drug targets according to their target binding affinities.

2.4. Molecular docking studies

The protein-ligand binding interaction of chosen protein-ligand complexes was performed using Autodock Vina (Trott and Olson, 2010). The docking analyses were performed using a semi-flexible docking approach. Briefly, proteins were kept rigid and ligands were kept flexible. The allowed degrees of freedom for ligand molecules were considered 10. The steps involving the conversion of molecules into pdbqt format, box type, grid box generation, etc. are specified by AutoDock. Since Remdesivir were considered as a potential drug for SARS-Cov2 based on some initial in-vitro findings (Shannon et al., 2020) and the site of interaction of the remdesivir to SARS-Cov2 RdRP has already been determined (Gao et al., 2020) we have chosen the interaction site for determining the inhibitory potential of the selected compounds in molecular docking. Critical 11 amino acid positions of A chain of RdRP (PDB ID: 6m71) is important for remdesivir binding and were selected for creating remdesivir incorporation model. These include K545, R553, R555, V557, D618, S 623, T680, D682, N691, D760 and D761. The grid box was set to size 22.32 Å × 23.91 Å × 32 .57 Å (x, y and z) parameters and the center 118.660 Å × 117.665 Å × 131.857 Å (x, y and z) parameters. The docking results were analyzed using Discovery studio visualizer (“BIOVIA Discovery Studio — Discngine,”) and Molecular Operating Environment (Vilar et al., 2008) software, and the docking of ligands RdRP with the least energy was considered to have a significant binding affinity.

2.5. Drug likeness analysis of the potential drug candidates:

ADMET profiling is a significant pointer in defining the effectiveness and safety of a drug compound before bringing it into commercialization. Due to cost-effectiveness and proper timing in the experimental evaluation of ADMET properties, computational methods have been developed as a practicable alternative in the high-throughput drug discovery process (Shen et al., 2010). The ADMET properties of the 8 top-ranked ligands were calculated by the online ADMET structure-activity database (admetSAR) (Yang et al., 2019) (http://lmmd.ecust.edu.cn/admetsar2/) and pkCSM (Pires et al., 2015) (http://biosig.unimelb.edu.au/pkcsm/) where SMILES (simplified molecular-input line-entry system) strings were utilized throughout the whole process.

2.6. Molecular dynamics simulation with MMGBSA scoring:

Complexes were solvated with TIP3P water model employing a dodecahedron box with a 12 Å packing using tleap available in Amber16 package (Case et al., 2005). The systems were then neutralized with Na^+ and Cl^- ions until neutrality. The protein, water molecules, and ions were defined by the ff14SB AMBER force field (Duan et al., 2003). Ligands were parameterized by assigning AM1-BCC atomic charges employing the General Amber force field (GAFF) (Wang et al., 2004). Simulations were run at the NPT ensemble at 310 K via a Langevin thermostat, 1 bar of pressure, and an isotropic Berendsen barostat. Periodic boundary conditions (PBC) were considered with a cutoff of 10 Å for the nonbonded interactions, whereas the electrostatic term was described via the PME method (Darden et al., 1993). A numeric time step of 2 fs and the SHAKE algorithm (Van Gunsteren and Berendsen, 1977) was chosen to constrain bond lengths at individual equilibrium. After constructions and previous MD simulations, a minimization and relaxing protocol was performed comprising of: 1,000 steps of energy minimization by conjugate gradient method; 1000 ps of pre-relaxation with harmonic restraint for protein and ligand; 1000 ps relaxation removing the ligand restrains; 1000 ps of relaxation with no restrictions to the side chains of the residues 5 Å around the ligand; 1000 ps of NPT relaxation without restrictions for the entire residues around the ligand; 50 ns of NPT MD simulations. The RMSD and clustering analysis was performed using the cpptraj tool in Amber16 to check system equilibration and identification of the most populated conformation during the MD simulations. Images were built using PyMOL (“DeLano, W.L. (2002) The PyMOL Molecular Graphics System. Delano Scientific, San Carlos. - References - Scientific Research Publishing,”).

The Molecular Mechanics Generalized Born Surface Area (MMGBSA) (Belouzard et al., 2012) approach was employed to determine the binding free energy (ΔGmmgbsa). This analysis was performed over the last 20 ns of MD simulation, selecting a total of 2000 snapshots at time intervals of 10 ps, using implicit solvent models (Feig et al., 2004), and a salt concentration of 0.10 M. The ΔGmmgbsa values were determined as previously described (Bello, 2018) and embody average values of triplicate MD simulations.

Results

3.1. Virtual screening, ligand selection and molecular docking studies

In order to identify potential drug candidates targeting SARS-CoV-2 RdRP we adopted a computational approach. Initially, with extensive literature mining, we selected 7 FDA-approved RdRP inhibitor drugs (Favipiravir (Allen et al., 2020), Sofosbuvir (Buonaguro and Buonaguro, 2020), Lopinavir (Chakraborty and Das, 2020), Tenofovir (Allen et al., 2020), Ribavirin (Gish, 2006), Ritonavir (Chakraborty and Das, 2020), Galidesivir (Allen et al., 2020) and Remdesivir (Fani et al., 2020) that are effective against broad ranges of RNA viruses, including past coronaviruses. We hypothesized that these inhibitor drugs and/or their structural homologues could have the potential to inhibit CoV-2 RdRP. Following downloading these drugs and their structural homologues (detailed in method section), we have performed an initial virtual screening using PyRx that eventually yielded 8 best compound hits. The structures of the 8 best compound hits are shown in **Figure 1.** To further validate the initial screen, we later performed molecular docking with AutoDock Vina (Trott and Olson, 2010) and the drug binding scores for the above mentioned approved drugs and their best hit homologues suggest high affinity binding (**Table 1 and Table 2)**, further strengthening our initial findings. It is important to mention that the structural homologues were predicted to have better binding than the existing FDA-approved drugs tested in this study, as evident from the binding scores (**Table 1 and Table 2)**.

3.2. Docking analyses and drug interactions

The chosen 8 compounds predicted (by molecular docking) to bind effectively with RdRP were selected for further analysis (the highest-ranked bound compound in all poses made as a cluster at the ligand-binding sites of these target protein). The analyses were performed target by target to check the efficiency of the ligand and the state of interaction using the Discovery studio visualizer ("BIOVIA Discovery Studio — Discngine,") and show that all the 8 ligands bind efficiently and interact well with RdRP (Figure 2).

3.3. Stability of simulated systems

The RMSD analysis plots show the mobility of the receptor-ligand complexes and constant values suggest that the system reached equilibrium (**Figure 3)**. The RMSD values of backbone atoms reached an equilibrium state between 20 to 30 ns with RMSD values that oscillated between 2.7 to 3.2 Å. Based on this, further analyses were performed considering the last 30 ns.

3.4. Structural analysis of receptor-ligand complexes

Analysis of the receptor-ligand complexes showed that 3 (ZINC000012863240, ZINC000049581065, and ZINC000072460420) out of 8 ligands lost interactions with the receptor at the beginning of the simulations, therefore, these three compounds were not considered in further analyses. Based on the simulation time in which systems reached equilibrium, a cluster analysis was performed using a cut-off of 2.5 Å to observe the main residues involving in stabilizing the ligand inside the binding site (**Figure 2**). The ligand orientation at the binding site is shown in **Figure 2**. ZINC000005605139 compound is coordinated by A524, R525, K591, R594, S652, and D730 through non-polar interactions. Whereas that T526 forms hydrogen bonds with compound through the polar backbone and side-chain atoms, as well as side chains of D422 and D593 (**Figure 4A**). ZINC000006094731 compound is bound by K515, Y516, A517, S519, K521, and R523 through non-polar interactions, whereas that R525 forms polar interactions through the backbone and side-chain atoms (**Figure 4B**). ZINC000012161475 compound is coupled through hydrophobic interactions with R523, W587, Y589, R594, N665, M725, D730, D731, A732, V733, V734, and F752, and forms polar interactions with D588 and K591 (**Figure 4C**). ZINC000014751834 is bound by S519, P590, M764, and K768 by hydrophobic contacts and polar interactions with backbone atoms of S765 (**Figure 4D**). ZINC000014882040 compound is coordinated through non-polar contacts with D422, Y425, R523, A524, R594, and K768, and polar interaction with side chains of K591 and N522, and with polar backbone atoms of A524 (**Figure 4E**). Comparative analysis revealed that most of the interactions are hydrophobic, and R523, A524, R525, and R594 residues were present in almost all the complexes, suggesting an important role of these residues in ligand binding stabilization.

3.5. Binding Free Energy of protein-ligand complexes

To further assess the thermodynamic feasibility of bind of the top-5 ligands to RdRP, MMGBSA method was used to calculate the binding free energy of the protein-ligand complex. Simulation runs were extracted to calculate the MMGBSA free binding energy. The results showed that five compounds showed negative binding free energy; suggesting successful binding throughout the simulation (**Table 3**). The molecular mechanic energy showed that Van der Waals energy (ΔEvdw + ΔGnpol, sol) was the main force for stabilizing the ligand at the binding site (**Table 3**)

3.6. ADMET properties

Drug bioavailability, metabolism and toxicity are important factors that may limit the use of a drug in clinical settings. Therefore, to determine whether the potential drug candidates are effectively bioavailable and have potentially no carcinogenicity to organs in human, the top-5 ligands were assessed based on their ADMET profile (**Table 4**) and all of the 5 drug candidates were found to have no potential toxicity (residing below toxicity classes of 4 and 5), which supports their safety for human use.

Finally, the top-5 screened ligands ZINC000005605139, ZINC000006094731, ZINC000012161475, ZINC000014751834, and ZINC000014882040 may be considered as potential therapeutic candidates for further exploring their potential in preclinical and clinical settings.

Discussion

The COVID-19 caused by rapidly spreading coronavirus, known as SARS-CoV-2 has been declared as a pandemic outbreak by WHO in March 2020. It has made a devastating impact on the public as well as the social health of more than 200 countries around the globe (https://www.who.int/emergencies/diseases/novel-coronavirus-2019). Therefore, scientific communities from all over the world have come forward to collaborate and

make the best effort for the earliest discovery of effective anti-viral drugs for treating COVID-19. The RdRP of SARS-CoV-2 has been sequenced and the X-ray crystallography 3-D structure is available in the PDB databank (Gao et al.).

Currently, there are no effective therapeutics for treating COVID-19. Therefore, the main focus has been on disease management with the focal point being, prevention of the infection and controlling measures. Recently, some anti-malarial drugs like chloroquine, hydroxychloroquine have given positive results *in vitro* cell culture systems but further clinical tests are needed for them to be approved as effective anti-viral drugs for treating SARS-CoV-2 infection (Enmozhi et al., 2020). A few other anti-viral drugs, including remdesivir, ribavirin etc., used for treating hepatitis C and Ebola virus disease and various vaccine candidates are being studied for effectively tackling the COVID-19 (Shoenfeld, 2020). Of particular interest was remdesivir; however, recently published clinical data showed no significant impact on the reduction in mortality, though the drug does reduce the recovery period (Hillaker et al., 2020).

Inhibition of the replication via inhibiting RdRP has been explored in the development of various antiviral drugs such as Favipiravir (Allen et al., 2020), Sofosbuvir (Buonaguro and Buonaguro, 2020), Lopinavir (Chakraborty and Das, 2020), Tenofovir (Allen et al., 2020), Ribavirin (Gish, 2006), Ritonavir (Chakraborty and Das, 2020), Galidesivir (Allen et al., 2020), and Remdesivir (Fani et al., 2020). Since there are no effective drugs for treating COVID-19, we adopted a computational approach to identify potential drug candidates. In this study, the inhibitory potential of the candidate drugs targeting SARS-CoV-2 RdRP was predicted via screening from a library of compounds of existing, approved drugs against RNA viruses and their structural analogues. Careful evaluation of the library by employing various computational screening methods yielded 5 candidate drugs and gave an insight into the potential of these prospective drugs against SARS-CoV-2.

The computational screening approach enables the rapid discovery of promising compounds for developing effective therapeutics against SARS CoV-2. It has been shown that less binding energy denotes more affinity of a compound for binding to its target (Ortiz et al., 1995). To elucidate the binding affinity to RdRP, the library of compounds was docked against RdRP using the PyRx tool (Dallakyan and Olson, 2015). Since among the approved RdRP drugs in clinical use the binding site of only remdesivir to SARS-Cov2 RdRP has already been elucidated as well as the in-vitro studies of remdesivir has showed some promises we selected 11 critical amino acids in RdRP pocket where the drug interacts. Compounds with a binding affinity of -7.5 Kcal/mol or less are evaluated as potent inhibitors of enzymatic mechanisms (R Yunta, 2016). Top ranked 8 compounds were selected based on their binding energy for further analysis. None of the approved drugs, including remdesivir, showed significant binding, perhaps these best hits are better candidates than the mother compounds.

The binding affinity determined from the docking study indicates the affinity of an individual ligand and the potency by which the ligand interacts and binds with the target protein at a specific pocket. For the best 8 hit compounds, our docking results were successful as they all were shown to have the least binding scores and presence of significant hydrogen bonding at the pocket of SARS-CoV-2 RdRP is detected. (**Table 2**; **Figure 2**).

Protein flexibility plays an essential role and should be considered when designing inhibitors against a target. Molecular docking has been performed implementing a single structure while MD simulation presents an in-depth interpretation of the protein-ligand interactions. RdRP, along with selected compounds, were used for molecular dynamics simulation analysis, which suggests that the ligand-bound receptor exhibit significant stability. Analysis of H-bond based interactions suggests that all of the compounds docked with the RdRP with all the available binding interactions and sustain all these interactions throughout the simulation process. Apart from that the receptor-ligand based interactions, all of the docked ligands on an average formed at least two H-bonds with the nearby water molecules, which bestowed further stability to the ligands docked.

MMGBSA analysis gave an insight into the binding energy throughout the simulation. The order of binding affinities of the finally selected 5 drug candidates are: ZINC000005605139 > ZINC000012161475 > ZINC000014882040 > ZINC000006094731 > ZINC000014751834. The other three compounds, ZINC000012863240, ZINC000049581065, and ZINC000072460420, were shown to be unstable inside the binding pocket of the SARS-CoV-2 RdRP. The more negative binding free energy (DGmmgbsa value) indicates the higher favorable binding, perhaps suggesting ZINC000005605139 and ZINC000012161475 these two compounds are better candidates to inhibit the enzyme compared to the other three compounds (Table 3).

ZINC000005605139 & ZINC000006094731, ZINC000012161475 & ZINC000014882040, ZINC000014751834 are structural analogues of Tenofovir, Lopinavir and Ritonavir respectively and this study predicted them to be more potent inhibitors of SARS-CoV-2 RdRP compared to the mother drugs.

Physicochemical properties of the selected compounds were studied using ADMET (Hodgson, 2001) to determine their drug-likeness properties. ADMET evaluates the molecular properties of a drug that are crucial for pharmacokinetics of the drug in human body, which includes absorption, distribution, metabolism, and excretion (ADME). Selected drugs showed satisfactory ADMET results as they are analogues of available drugs suggesting that safety and efficacy have already been proven. Although 4 of the 5 compounds show hepatotoxicity as predicted from ADMET, however, the level of toxicity to the liver, if any, needs to be addressed in preclinical and clinical settings.

Conclusion

The present *in silico* investigation explored the potentiality of the analogues of the available drugs in inhibiting SARS-CoV-2 RdRP. The result of the virtual screening yielded top-5 hit ligands. An ideal drug is presumed to not only have a high affinity to a specific target but should also have the drug likeness properties. Taking into account, for better prediction, the binding affinities predicted by MMGBSA, binding modes and further 50 ns MD simulation were also determined, and five ligands (ZINC000005605139, ZINC000006094731 ZINC000012161475, ZINC000014751834, and ZINC000014882040) were found to be the most favorable ones. Considering the safety issue of these drugs, all five compounds showed a good ADMET profile. The identified 5 drug candidates may have therapeutic potential in COVID-19. The analysis, however, offers further preclinical and clinical investigation to proof their efficacy against SARS-CoV-2.

Declarations

Funding:

No funding from any public, private or non-profit research agency was received for this study.

Declaration of interest:

The authors report no conflicts of interest. The authors alone are responsible for the content and writing of this article.

Acknowledgements:

The authors acknowledge Saeed Anwar (University of Alberta) and Sohel Mahmud (Tejgaon College, National University of Bangladesh) for helping with the writing of the manuscript.

References

Adams, P.D., Afonine, P. V., Bunkóczi, G., Chen, V.B., Davis, I.W., Echols, N., Headd, J.J., Hung, L.W., Kapral, G.J., Grosse-Kunstleve, R.W., McCoy, A.J., Moriarty, N.W., Oeffner, R., Read, R.J., Richardson, D.C., Richardson, J.S., Terwilliger, T.C., Zwart, P.H., 2010. PHENIX: A comprehensive Python-based system for macromolecular structure solution. Acta Crystallogr. Sect. D Biol. Crystallogr. 66, 213–221. https://doi.org/10.1107/S0907444909052925

Ahmed, S., Mahtarin, R., Ahmed, S.S., Akter, S., Islam, M.S., Mamun, A. Al, Islam, R., Hossain, M.N., Ali, M.A., Sultana, M.U.C., Parves, M.R., Ullah, M.O., Halim, M.A., 2020. Investigating the binding affinity, interaction, and structure-activity-relationship of 76 prescription antiviral drugs targeting RdRp and Mpro of SARS-CoV-2. J. Biomol. Struct. Dyn. 1–16. https://doi.org/10.1080/07391102.2020.1796804

Allen, C., Arjona, S., Santerre, M., Sawaya, B. e, 2020. OSF | Potential use of RNA-dependent RNA polymerase (RdRp) inhibitor against COVID-19 infection.

Beigel, J.H., Tomashek, K.M., Dodd, L.E., Mehta, A.K., Zingman, B.S., Kalil, A.C., Hohmann, E., Chu, H.Y., Luetkemeyer, A., Kline, S., Lopez de Castilla, D., Finberg, R.W., Dierberg, K., Tapson, V., Hsieh, L., Patterson, T.F., Paredes, R., Sweeney, D.A., Short, W.R., Touloumi, G., Lye, D.C., Ohmagari, N., Oh, M., Ruiz-Palacios, G.M., Benfield, T., Fätkenheuer, G., Kortepeter, M.G., Atmar, R.L., Creech, C.B., Lundgren, J., Babiker, A.G., Pett, S., Neaton, J.D., Burgess, T.H., Bonnett, T., Green, M., Makowski, M., Osinusi, A., Nayak, S., Lane, H.C., 2020. Remdesivir for the Treatment of Covid-19 — Preliminary Report. N. Engl. J. Med. https://doi.org/10.1056/nejmoa2007764

Bello, M., 2018. Binding mechanism of kinase inhibitors to EGFR and T790M, L858R and L858R/T790M mutants through structural and energetic analysis. Int. J. Biol. Macromol. 118, 1948–1962. https://doi.org/10.1016/j.ijbiomac.2018.07.042

Belouzard, S., Millet, J.K., Licitra, B.N., Whittaker, G.R., 2012. Mechanisms of coronavirus cell entry mediated by the viral spike protein. Viruses 4, 1011–1033. https://doi.org/10.3390/v4061011

BIOVIA Discovery Studio — Discngine [WWW Document], n.d. URL https://www.discngine.com/discovery-studio?fbclid=IwAR03C1rUwjrGm35Bhp41SGS-lDRxGOXlxbo-Pw7bFPS1EVqABwZmj4gGz_Q (accessed 9.19.20).

Blair, W., Cox, C., 2016. Current Landscape of Antiviral Drug Discovery. F1000Research 5. https://doi.org/10.12688/f1000research.7665.1

Brinks, V., Ibert, O., 2020. From Corona Virus to Corona Crisis: The Value of An Analytical and Geographical Understanding of Crisis. Tijdschr. voor Econ. en Soc. Geogr. 111, 275–287. https://doi.org/10.1111/tesg.12428

Buonaguro, L., Buonaguro, F.M., 2020. Knowledge-based repositioning of the anti-HCV direct antiviral agent Sofosbuvir as SARS-CoV-2 treatment. Infect. Agent. Cancer 15. https://doi.org/10.1186/s13027-020-00302-x

Case, D.A., Cheatham, T.E., Darden, T., Gohlke, H., Luo, R., Merz, K.M., Onufriev, A., Simmerling, C., Wang, B., Woods, R.J., 2005. The Amber biomolecular simulation programs. J. Comput. Chem. 26, 1668–1688. https://doi.org/10.1002/jcc.20290

Chakraborty, S., Das, G., 2020. Why re-purposing HIV drugs Lopinavir/ritonavir to inhibit the SARS-Cov2 protease probably wont work - but re-purposing Ribavirin might since it has a very similar binding site within the RNA-polymerase. https://doi.org/10.31219/osf.io/ax98f

Coronavirus Update (Live): 46,210,349 Cases and 1,197,805 Deaths from COVID-19 Virus Pandemic - Worldometer [WWW Document], n.d. URL https://www.worldometers.info/coronavirus/ (accessed 11.1.20).

Dallakyan, S., Olson, A.J., 2015. Small-molecule library screening by docking with PyRx. Methods Mol. Biol. 1263, 243–250. https://doi.org/10.1007/978-1-4939-2269-7_19

Darden, T., York, D., Pedersen, L., 1993. Particle mesh Ewald: An N·log(N) method for Ewald sums in large systems. J. Chem. Phys. 98, 10089–10092. https://doi.org/10.1063/1.464397

DeLano, W.L. (2002) The PyMOL Molecular Graphics System. Delano Scientific, San Carlos. - References - Scientific Research Publishing [WWW Document], n.d. URL https://www.scirp.org/(S(vtj3fa45qm1ean45vvffcz55))/reference/ReferencesPapers.aspx?ReferenceID=1958992 (accessed 9.20.20).

Duan, Y., Wu, C., Chowdhury, S., Lee, M.C., Xiong, G., Zhang, W., Yang, R., Cieplak, P., Luo, R., Lee, T., Caldwell, J., Wang, J., Kollman, P., 2003. A Point-Charge Force Field for Molecular Mechanics Simulations of Proteins Based on Condensed-Phase Quantum Mechanical Calculations. J. Comput. Chem. 24, 1999–2012. https://doi.org/10.1002/jcc.10349

Elfiky, A.A., 2020. Ribavirin, Remdesivir, Sofosbuvir, Galidesivir, and Tenofovir against SARS-CoV-2 RNA dependent RNA polymerase (RdRp): A molecular docking study. Life Sci. 253, 117592. https://doi.org/10.1016/j.lfs.2020.117592

Enmozhi, S.K., Raja, K., Sebastine, I., Joseph, J., 2020. Andrographolide As a Potential Inhibitor of SARS-CoV-2 Main Protease: An In Silico Approach. J. Biomol. Struct. Dyn. 1–10. https://doi.org/10.1080/07391102.2020.1760136

Fani, M., Teimoori, A., Ghafari, S., 2020. Comparison of the COVID-2019 (SARS-CoV-2) pathogenesis with SARS-CoV and MERS-CoV infections. Future Virol. 15, 317–323. https://doi.org/10.2217/fvl-2020-0050

Feig, M., Onufriev, A., Lee, M.S., Im, W., Case, D.A., Brooks, C.L., 2004. Performance Comparison of Generalized Born and Poisson Methods in the Calculation of Electrostatic Solvation Energies for Protein Structures. J. Comput. Chem. 25, 265–284. https://doi.org/10.1002/jcc.10378

Gao, Y., Yan, L., Huang, Y., Liu, F., Zhao, Y., Cao, L., Wang, T., Sun, Q., Ming, Z., Zhang, L., Ge, J., Zheng, L., Zhang, Y., Wang, H., Zhu, Y., Zhu, C., Hu, T., Hua, T., Zhang, B., Yang, X., Li, J., Yang, H., Liu, Z., Xu, W., Guddat, L.W., Wang, Q., Lou, Z., Rao, Z., 2020. Structure of the RNA-dependent RNA polymerase from COVID-19 virus. Science (80-.). 368, 779–782. https://doi.org/10.1126/science.abb7498

Gao, Y., Yan, L., Huang, Y., Liu, F., Zhao, Y., Cao, L., Wang, T., Sun, Q., Ming, Z., Zhang, L., Ge, J., Zheng, L., Zhang, Y., Wang, H., Zhu, Y., Zhu, C., Hu, T., Hua, T., Zhang, B., Yang, X., Li, J., Yang, H., Liu, Z., Xu, W., Guddat, L.W., Wang, Q., Lou, Z., Rao, Z., n.d. RCSB PDB - 6M71: SARS-Cov-2 RNA-dependent RNA polymerase in complex with cofactors [WWW Document]. URL https://www.rcsb.org/structure/6M71 (accessed 9.30.20).

Gish, R.G., 2006. Treating HCV with ribavirin analogues and ribavirin-like molecules. J. Antimicrob. Chemother. 57, 8–13. https://doi.org/10.1093/jac/dki405

Guex, N., Peitsch, M.C., 1997. SWISS-MODEL and the Swiss-PdbViewer: An environment for comparative protein modeling. Electrophoresis 18, 2714–2723. https://doi.org/10.1002/elps.1150181505

Harrison, C., 2020. Coronavirus puts drug repurposing on the fast track. Nat. Biotechnol. 38, 379–381. https://doi.org/10.1038/d41587-020-00003-1

Hillaker, E., Belfer, J.J., Bondici, A., Murad, H., Dumkow, L.E., 2020. Delayed Initiation of Remdesivir in a COVID-19-Positive Patient. Pharmacotherapy 40, 592–598. https://doi.org/10.1002/phar.2403

Hodgson, J., 2001. ADMET - Turning chemicals into drugs. Rapidly resolving the pharmacokinetic and toxicological properties of drug candidates remains a key challenge for drug developers. Nat. Biotechnol. 19, 722–726. https://doi.org/10.1038/90761

Hofmann, W.P., Herrmann, E., Sarrazin, C., Zeuzem, S., 2008. Ribavirin mode of action in chronic hepatitis C: from clinical use back to molecular mechanisms. Liver Int. 28, 1332–1343. https://doi.org/10.1111/j.1478-3231.2008.01896.x

Huang, C., Wang, Y., Li, X., Ren, L., Zhao, J., Hu, Y., Zhang, L., Fan, G., Xu, J., Gu, X., Cheng, Z., Yu, T., Xia, J., Wei, Y., Wu, W., Xie, X., Yin, W., Li, H., Liu, M., Xiao, Y., Gao, H., Guo, L., Xie, J., Wang, G., Jiang, R., Gao, Z., Jin, Q., Wang, J., Cao, B., 2020. Clinical features of patients infected with 2019 novel coronavirus in Wuhan, China. Lancet 395, 497–506. https://doi.org/10.1016/S0140-6736(20)30183-5

JC, K., KL, S., MA, C., 2018. Acute Myocardial Infarction after Laboratory-Confirmed Influenza Infection. N. Engl. J. Med. 378, 2538–2541. https://doi.org/10.1056/nejmc1805679

Li, G., De Clercq, E., 2020. Therapeutic options for the 2019 novel coronavirus (2019-nCoV). Nat. Rev. Drug Discov. 19, 149–150. https://doi.org/10.1038/d41573-020-00016-0

Li, Z., Wu, M., Yao, J., Guo, J., Liao, X., Song, S., Li, J., Duan, G., Zhou, Yuanxiu, Wu, X., Zhou, Z., Wang, T., Hu, M., Chen, Xianxiang, Fu, Y., Lei, C., Dong, H., Xu, C., Hu, Y., Han, M., Zhou, Yi, Jia, H., Chen, Xiaowei, Yan, J., 2020. Caution on Kidney Dysfunctions of COVID-19 Patients. SSRN Electron. J. 2020.02.08.20021212. https://doi.org/10.1101/2020.02.08.20021212

Lin, M.I., Su, B.H., Lee, C.H., Wang, S.T., Wu, W.C., Dangate, P., Wang, S.Y., Huang, W.I., Cheng, T.J., Lin, O.A., Cheng, Y.S.E., Tseng, Y.J., Sun, C.M., 2015. Synthesis and inhibitory effects of novel pyrimido-pyrrolo-quinoxalinedione analogues targeting nucleoproteins of influenza A virus H1N1. Eur. J. Med. Chem. 102, 477–486. https://doi.org/10.1016/j.ejmech.2015.08.016

Ludwig, S., Zarbock, A., 2020. Coronaviruses and SARS-CoV-2: A Brief Overview. Anesth. Analg. 93–96. https://doi.org/10.1213/ANE.0000000000004845

Lung, J., Lin, Y., Yang, Y., Chou, Y., Shu, L., Cheng, Y., Liu, H. Te, Wu, C., 2020. The potential chemical structure of anti-SARS-CoV-2 RNA-dependent RNA polymerase. J. Med. Virol. 92, 693–697. https://doi.org/10.1002/jmv.25761

Mitjà, O., Clotet, B., 2020. Use of antiviral drugs to reduce COVID-19 transmission. Lancet Glob. Heal. 8, e639–e640. https://doi.org/10.1016/S2214-109X(20)30114-5

Nguyen, J.L., Yang, W., Ito, K., Matte, T.D., Shaman, J., Kinney, P.L., 2016. Seasonal influenza infections and cardiovascular disease mortality. JAMA Cardiol. 1, 274–281. https://doi.org/10.1001/jamacardio.2016.0433

Ortiz, A.R., Pisabarro, M.T., Gago, F., Wade, R.C., 1995. Prediction of Drug Binding Affinities by Comparative Binding Energy Analysis. J. Med. Chem. 38, 2681–2691. https://doi.org/10.1021/jm00014a020

Pires, D.E.V., Blundell, T.L., Ascher, D.B., 2015. pkCSM: Predicting small-molecule pharmacokinetic and toxicity properties using graph-based signatures. J. Med. Chem. 58, 4066–4072. https://doi.org/10.1021/acs.jmedchem.5b00104

R Yunta, M.J., 2016. Docking and Ligand Binding Affinity: Uses and Pitfalls. Am. J. Model. Optim. 4, 74–114. https://doi.org/10.12691/ajmo-4-3-2

Shannon, A., Le, N.T.T., Selisko, B., Eydoux, C., Alvarez, K., Guillemot, J.C., Decroly, E., Peersen, O., Ferron, F., Canard, B., 2020. Remdesivir and SARS-CoV-2: Structural requirements at both nsp12 RdRp and nsp14 Exonuclease active-sites. Antiviral Res. 178. https://doi.org/10.1016/j.antiviral.2020.104793

Shen, J., Cheng, F., Xu, Y., Li, W., Tang, Y., 2010. Estimation of ADME properties with substructure pattern recognition. J. Chem. Inf. Model. 50, 1034–1041. https://doi.org/10.1021/ci100104j

Shoenfeld, Y., 2020. Corona (COVID-19) time musings: Our involvement in COVID-19 pathogenesis, diagnosis, treatment and vaccine planning. Autoimmun. Rev. 19. https://doi.org/10.1016/j.autrev.2020.102538

Şimşek Yavuz, S., Ünal, S., 2020. Antiviral treatment of covid-19. Turkish J. Med. Sci. 50, 611–619. https://doi.org/10.3906/sag-2004-145

Sinha, N., Balayla, G., 2020. Hydroxychloroquine and covid-19. Postgrad. Med. J. 96, 550–555. https://doi.org/10.1136/postgradmedj-2020-137785

Slaoui, M., Hepburn, M., 2020. Developing Safe and Effective Covid Vaccines — Operation Warp Speed's Strategy and Approach. N. Engl. J. Med. https://doi.org/10.1056/nejmp2027405

Sterling, T., Irwin, J.J., 2015. ZINC 15 - Ligand Discovery for Everyone. J. Chem. Inf. Model. 55, 2324–2337. https://doi.org/10.1021/acs.jcim.5b00559

Tai, W., He, L., Zhang, X., Pu, J., Voronin, D., Jiang, S., Zhou, Y., Du, L., 2020. Characterization of the receptor-binding domain (RBD) of 2019 novel coronavirus: implication for development of RBD protein as a viral attachment inhibitor and vaccine. Cell. Mol. Immunol. 17, 613–620. https://doi.org/10.1038/s41423-020-0400-4

Trott, O., Olson, A.J., 2010. AutoDock Vina: Improving the speed and accuracy of docking with a new scoring function, efficient optimization, and multithreading. J. Comput. Chem. 31, 455–61. https://doi.org/10.1002/jcc.21334

Van Gunsteren, W.F., Berendsen, H.J.C., 1977. Algorithms for macromolecular dynamics and constraintdynamics. Mol. Phys. 34, 1311–1327. https://doi.org/10.1080/00268977700102571

Van Kampen, J.J.A., Van De Vijver, D.A.M.C., Fraaij, P.L.A., Haagmans, B.L., Lamers, M.M., Sc, M., Okba, N., Van Den Akker, J.P.C., Endeman, H., Gommers, D.A.M.P.J., Cornelissen, J.J., Hoek, R.A.S., Van Der Eerden, M.M., Hesselink, D.A., Metselaar, H.J., Verbon, A., De Steenwinkel, J.E.M., Aron, G.I., Van Gorp, E.C.M., Van Boheemen, S., Voermans, J.C., Boucher, C.A.B., Molenkamp, R., Koopmans, M.P.G., Geurtsvankessel, C., Van Der Eijk, A.A., 2020. Shedding of infectious virus in hospitalized patients with coronavirus disease-2019 (COVID-19): duration and key determinants. medRxiv 2020.06.08.20125310. https://doi.org/10.1101/2020.06.08.20125310

Vilar, S., Cozza, G., Moro, S., 2008. Medicinal Chemistry and the Molecular Operating Environment (MOE): Application of QSAR and Molecular Docking to Drug Discovery. Curr. Top. Med. Chem. 8, 1555–1572. https://doi.org/10.2174/156802608786786624

Wang, J., Wolf, R.M., Caldwell, J.W., Kollman, P.A., Case, D.A., 2004. Development and testing of a general Amber force field. J. Comput. Chem. 25, 1157–1174. https://doi.org/10.1002/jcc.20035

Woo, P.C.Y., Huang, Y., Lau, S.K.P., Yuen, K.Y., 2010. Coronavirus genomics and bioinformatics analysis. Viruses 2, 1805–1820. https://doi.org/10.3390/v2081803

Yang, H., Lou, C., Sun, L., Li, J., Cai, Y., Wang, Z., Li, W., Liu, G., Tang, Y., 2019. AdmetSAR 2.0: Web-service for prediction and optimization of chemical ADMET properties. Bioinformatics 35, 1067–1069. https://doi.org/10.1093/bioinformatics/bty707

Zhang1, L., Zhou1, R., 2020. Binding Mechanism of Remdesivir to SARS-CoV-2 RNA Dependent RNA Polymerase. Prepr. | NOT PEER-REVIEWED | Posted. https://doi.org/10.20944/preprints202003.0267.v1

Zoete, V., Daina, A., Bovigny, C., Michielin, O., 2016. SwissSimilarity: A Web Tool for Low to Ultra High Throughput Ligand-Based Virtual Screening. J. Chem. Inf. Model. 56, 1399–1404. https://doi.org/10.1021/acs.jcim.6b00174

Tables

Table 1. Autodock Vina docking results of the selected antiviral drugs

Compound	PMCID	Score (KJ/mol)
Remdesivir	121304016	-6.5
Lopinavir	92727	-7
Ribavirin	37542	-6.2
Galidesivir	10445549	-6.8
Sofosbuvir	45375808	-7.5
Favipiravir	492405	-5.5
Tenofovir	464205	-5.9
Ritonavir	392622	-7.2

Table 2. Autodock Vina docking results of the top-ranking ligands

Compound	IUPAC name	Score (KJ/mol)
ZINC000005605139	4-Amino-N'-naphthalen-2-ylsulfonyl-1,2,5-oxadiazole-3- carbohydrazide	-7.9
ZINC000006094731	(7R,8R,9S,10S)-7,8,10-Trihydroxy-7,8,9,10-tetrahydrobenzo[a]pyrene-9-sulfonic acid	-8.1
ZINC000012161475	5-[1-(2-Naphthalen-2-ylacetyl)piperidin-4-yl]-3-(oxolan-2-ylmethyl)-5-propylimidazolidine-2,4-dione	-8.9
ZINC000014751834	[3-(4-Hydroxypiperidine-1-carbonyl)-1-(2-phenylethyl)-6,7-dihydro-4H-pyrazolo[4,3-c]pyridin-5-yl]-(1H-indol-5-yl)methanone	-8.9
ZINC000014882040	5-[(4-Fluorophenyl)methyl]-5-[1-[2-(3-methylphenyl) acetyl]piperidin-4-yl]-3-(oxolan-3-yl)imidazolidine-2,4-dione	-9.1
ZINC000012863240	N-[1-(4a-Hydroxy-1,3,4,5,6,7,8,8a-octahydroisoquinolin-2-yl)-3-(1H-indol-3-yl)-1-oxopropan-2-yl]-4-methylbenzenesulfonamide	-9.1
ZINC000049581065	N'-(1,3-Diphenylpyrazole-4-carbonyl)-3-(2-hydroxyethyl)-4-oxophthalazine-1-carbohydrazide	-9.1
ZINC000072460420	7-(3,4-Dihydro-2H-1,5-benzodioxepin-7-yl)-2-(hydroxymethyl)-5-methyl-N-phenyl-1,7-dihydro[1,2,4]triazolo[1,5-a]pyrimidine-6-carboxamide	-8.6

Table 3. Binding free energy components of protein-ligand systems (in units of kcal/mol).

System	ΔE_{vdw}	ΔE_{ele}	$\Delta G_{ele,sol}$	$\Delta G_{npol,sol}$	DG_{mmgbsa}
ZINC000005605139	-31.90 ± 4.0	-191.27 ± 13.5	186.38 ± 12.6	-4.92 ± 0.40	-41.72 ± 4.0
ZINC000006094731	-29.08 ± 3.0	-18.76 ± 6.5	30.18 ± 12.0	-3.76 ± 0.40	-21.43 ± 6.0
ZINC000012161475	-50.73 ± 4.0	-32.16 ± 7.5	52.51 ± 6.4	-5.99 ± 0.50	-36.40 ± 5.0
ZINC000014751834	-29.79 ± 4.0	-35.13 ± 11.0	48.54 ± 8.0	-4.09 ± 0.70	-20.47 ± 5.0
ZINC000014882040	-34.84 ± 6.0	-33.81 ± 10.7	48.09 ± 9.7	-4.87 ± 0.70	-25.43 ± 6.0

Table 4. ADMET results of the top-ranking ligands

Property	Model Name	ZINC000005605139	ZINC000006094731	ZINC000012161475	ZINC000014751834	ZINC0000148820
Absorption	Water solubility	-3.533	-2.891	-5.178	-4.127	-4.263
Absorption	Caco2 permeability	0.492	1.237	0.846	1.307	1.159
Absorption	Intestinal absorption (human)	72.698	39.7	95.097	87.731	90.718
Distribution	BBB permeability	-1.118	-1.353	-0.979	-0.69	-0.638
Distribution	CNS permeability	-3.219	-3.176	-2.419	-2.453	-2.471
Metabolism	CYP1A2 inhibitor	No	No	No	No	No
Metabolism	CYP2C19 inhibitior	No	No	Yes	Yes	Yes
Metabolism	CYP2C9 inhibitior	No	No	Yes	Yes	Yes
Metabolism	CYP2D6 inhibitior	No	No	No	No	No
Metabolism	CYP3A4 inhibitior	No	No	Yes	Yes	Yes
Toxicity	AMES toxicity	No	No	No	No	No
Toxicity	Hepatotoxicity	Yes	No	Yes	Yes	Yes

Figures

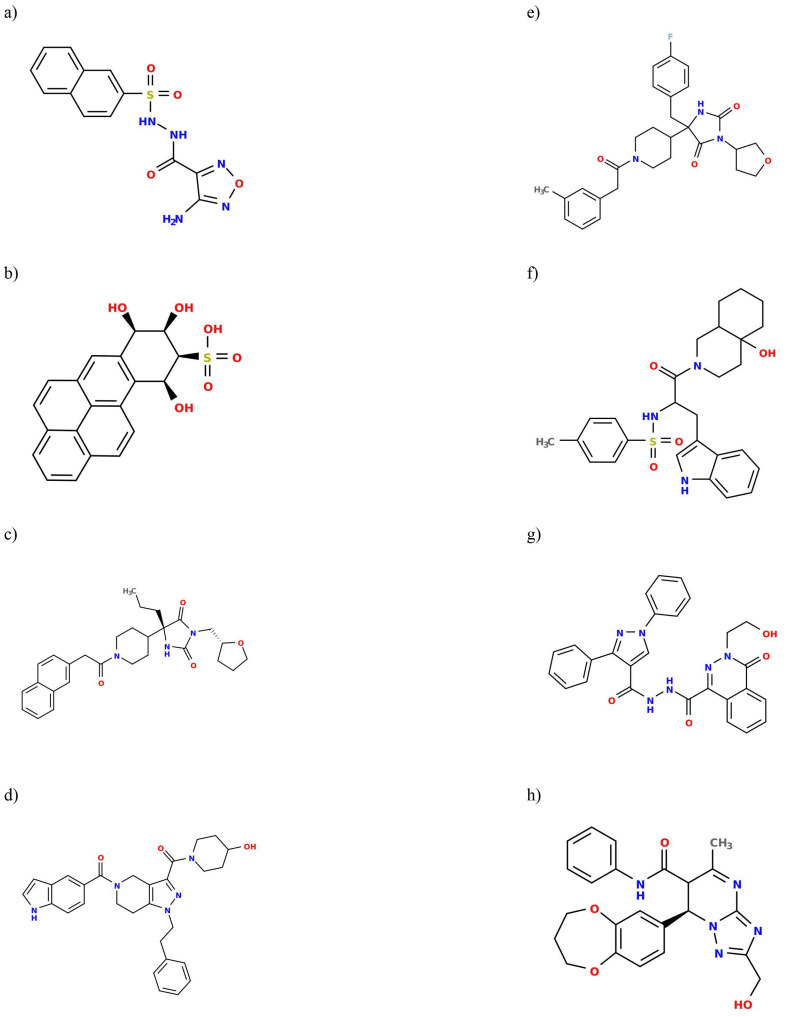

Figure 1

The chemical structures of ligands that were selected based on the initial virtual screen. a) ZINC000005605139, b) ZINC000006094731, c) ZINC000012161475, d) ZINC000014751834 and e) ZINC000014882040, f) ZINC000012863240, g) ZINC000049581065, h) ZINC000072460420.

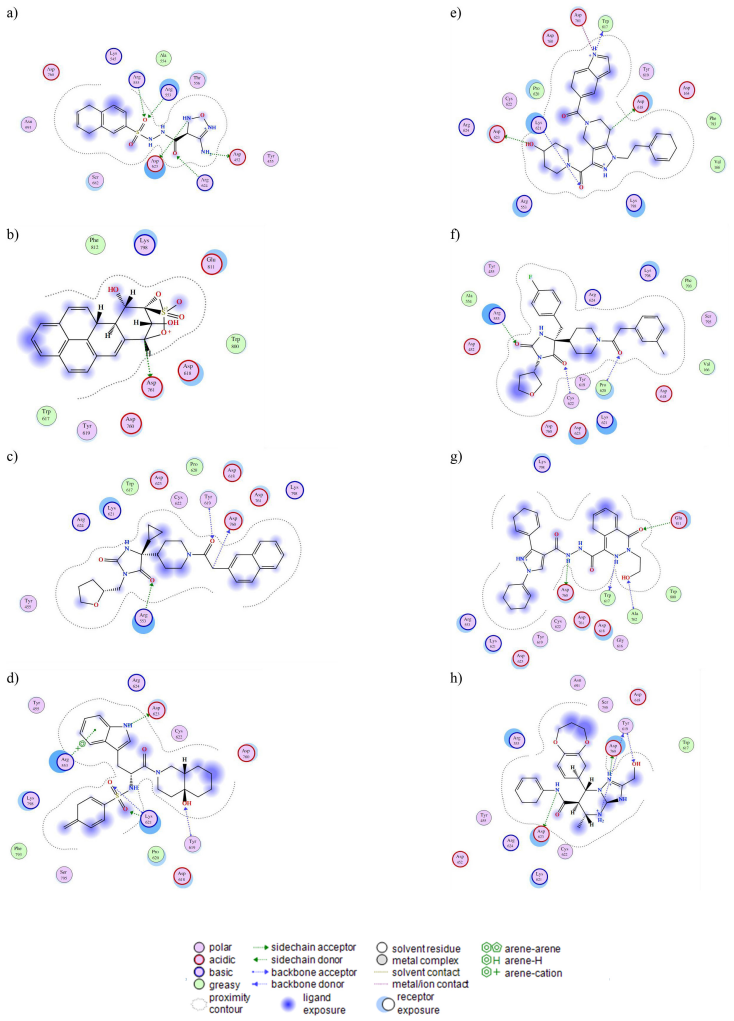

Figure 2

Molecular docking of probable inhibitory molecules onto RdRp. Panels (a–h) show the 2D structures of the binding interaction of the ligands inside the pocket of SARS Cov-2 RdRp a) ZINC000005605139, b) ZINC000006094731, c) ZINC000012161475, d) ZINC000014751834 and e) ZINC000014882040, f) ZINC000012863240, g) ZINC000049581065, h) ZINC000072460420. The types of interaction are shown at the end of the figure.

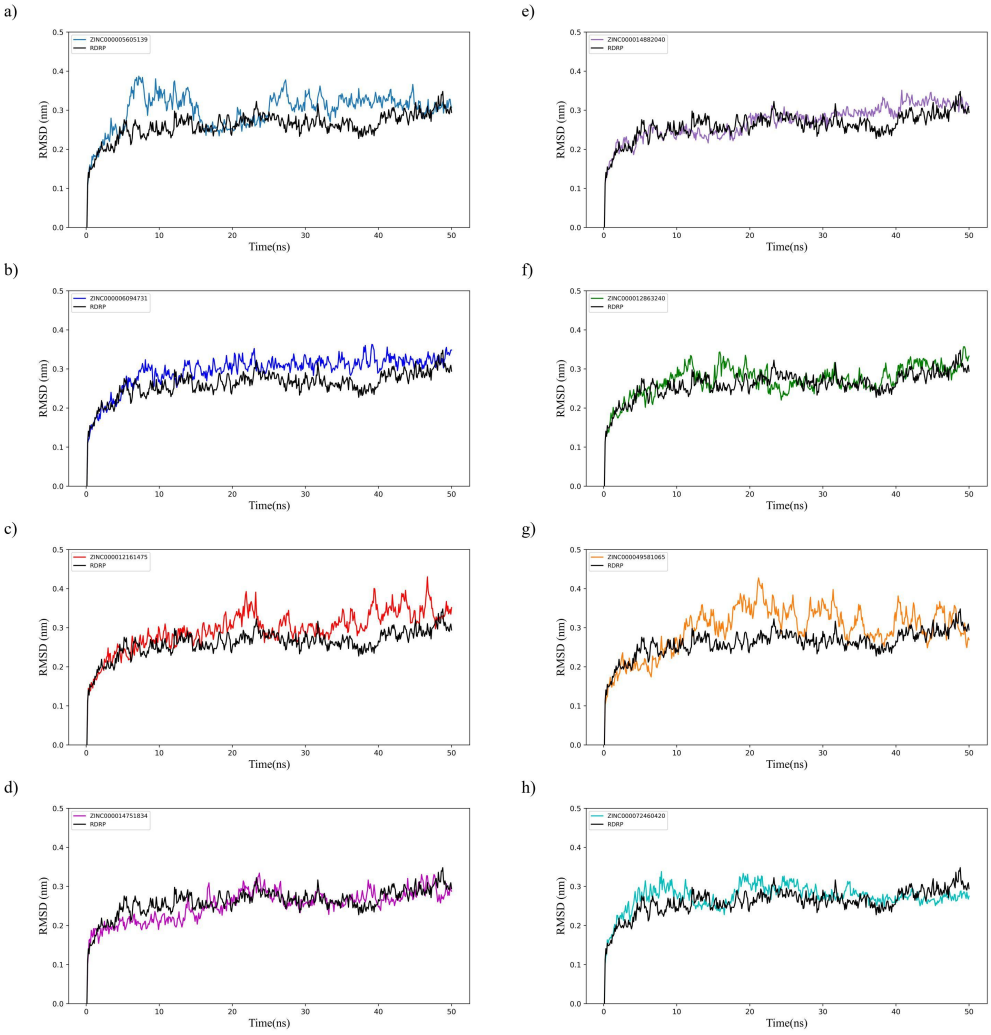

Figure 3

RMSD pattern of docked complexes compared to Cov-2 RdRp. a) ZINC000005605139, b) ZINC000006094731, c) ZINC000012161475, d) ZINC000014751834 and e) ZINC000014882040, f) ZINC000012863240, g) ZINC000049581065, h) ZINC000072460420. The RMSD pattern show that all the small molecules docked to the RdRp protein remain relatively stable under the simulated environment.

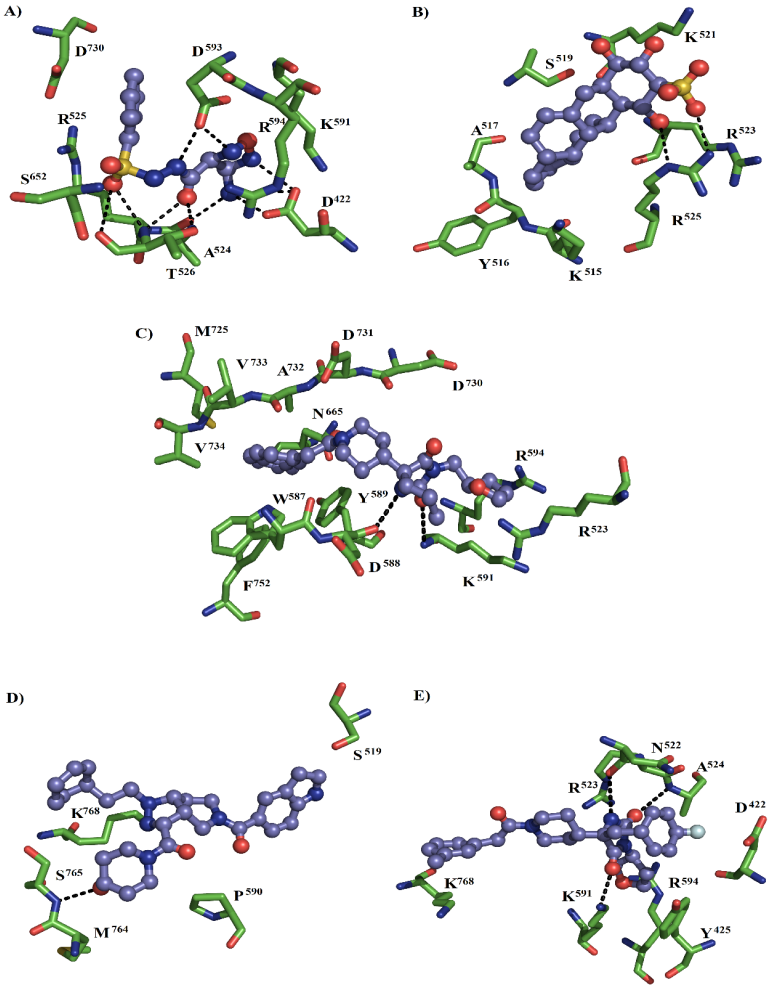

Figure 4

The binding orientation of 5 best ligands inside the receptor binding site of SARS Cov-2 RdRp. A) ZINC000005605139, B) ZINC000006094731, C) ZINC000012161475, D) ZINC000014751834 and E) ZINC000014882040. The binding orientation indicates stable binding for each of the 5 ligands to the RdRp of Cov-2.